Biomedical Signal Processing and Control 66 (2021) 102504

Contents lists available at ScienceDirect

Biomedical Signal Processing and Control

journal homepage: www.elsevier.com/locate/bspc

Subspace-based feature extraction on multi-physiological measurements of automobile drivers for distress recognition

Idil Isikli Esener

Department of Electrical Electronics Engineering, Bilecik Seyh Edebali University, 11210, Bilecik, Turkey

ARTICLE INFO

Keywords:
Stress recognition
Intelligent transport systems
Discriminative common vector
Support vector machines

ABSTRACT

The automotive industry has accelerated the utilization of Intelligent Transport Systems (ITS) in vehicles for increased driving safety. In this paper, a novel and well-done subspace feature extraction scheme on the physiological signals acquired by wearable sensors, for drivers' distress level detection to be introduced as an ITS is proposed and verified on the publicly available MIT-BIH PhysioNet Multi-parameter Database. The proposed scheme includes two phases where time-domain statistical feature extraction is first realized on the electrocardiogram (ECG), hand galvanic skin response (hand GSR), foot galvanic skin response (foot GSR), electromyogram (EMG), and respiration (RESP) signals, and secondly subspace feature vector construction is appreciated by applying Discriminative Common Vector (DCV) decomposition on the statistical feature vectors. The distress levels of the drivers are determined as low, moderate, and high by utilizing both the statistical and the subspace feature vectors using Support Vector Machines (SVM) classifier by 2-fold cross-validation technique. A maximum of 88.89 % classification accuracy is achieved using statistical features in 7384 s while it is increased to 100 % in 3,421 s when subspace features are employed. The increased classification accuracy in decreased time consumption evidently shows the success of the proposed feature extraction scheme.

1. Introduction

In recent years, stress has been the subject of many studies as being one of the most common problems of modern life. Distress (negative stress) is defined as the negative emotions and unexpected behaviors of any individual as a result of physical and emotional disruption in his physical and social environment [1]. Distress is categorized into three types as acute, episodic acute and chronic stress according to its physical, emotional, mental and behavioral effects, duration of these effects and the treatment approaches [2]. Acute stress is defined as the short-term stress state caused by daily life stressors related to recent past or near future [3]. Episodic acute stress is caused by recurrence of acute stress frequently while chronic stress is the long-term stress state caused by gradual increase in acute stress as a result of inability to relax [3].

The physical, mental, and behavioral effects of distress can adversely affect the driver performance, resulting in traffic violations and accidents [4,5]. Although driving performance of professional drivers, suffering from chronic stress, can be negatively affected due to their high mental workload [3,6] and negative mood [3,7], drivers are most probably influenced by acute or episodic acute stress caused by sudden changes in driving conditions due to road conditions, traffic density, social interactions, unexpected situations, other drivers' or pedestrians' behaviors, events that impact time schedule, and difficult driving due to urban planning [3,8].

In this day and age, the use of computer-aided systems, namely Intelligent Transport Systems (ITS), in new generation vehicles gain importance in parallel with the development of computer and automotive technologies. ITS include systems that increase the safety against possible traffic accidents, such as lane departure warning system, fatigue detection system, and collision notification and avoidance. In addition to these, since the organizational or social stress pushed on one's shoulder directly affects the driving safety, it is foresighted that the use of a system in vehicles that can detect the drivers' stress level will be an effective prevention against traffic violations and accidents.

Acute stress is physiologically characterized by increments in blood sugar level, respiration rate, number of heartbeat, blood pressure, and muscle activity; shortness of breath, sweaty palms, cold hands or feet, dizziness, chest pain, headache, activation of the blood coagulation mechanism, irritable bowel syndrome or pupil dilation, by stimulating the sympathetic nervous system [9]. Relevant information on these effects can be measured by physiological sensors including electrocardiogram (ECG), galvanic skin response (GSR), electromyogram (EMG),

E-mail address: idil.isikli@bilecik.edu.tr.

https://doi.org/10.1016/j.bspc.2021.102504
Received 27 March 2019; Received in revised form 30 January 2021; Accepted 9 February 2021
Available online 20 February 2021

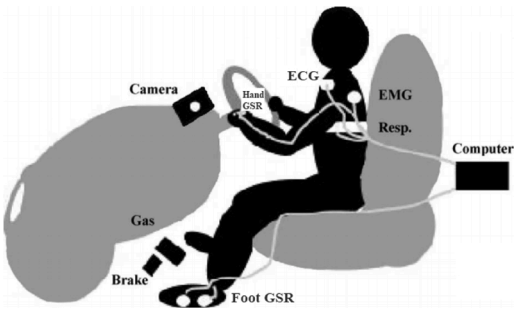

Fig. 1. Physiological signal collection [15].

and respiration (RESP) [10].

Most studies in the literature focus on the usage of physiological measurements for drivers' distress level detection. These studies consist of physiological feature extraction schemes in time-domain [11–14], time- and Fourier-domain [10,15–21], and time-, Fourier-, and wavelet-domain [22]. In addition to the studies utilizing only physiological measurements, feature ensembles constructed by concatenating physiological features by video-based features [23] and mechanical information of the vehicle [24].

Heart rate variability, thought to be an important sign of stress, is computed as the rate of the energy of the low frequency band of the ECG signal over the energy of the high frequency band [15,16,18,19,21–23]. Along with this rate, the power spectrum of ECG [10,17,19,21–23], EMG [20], GSR [18], and RESP [10,15,17] signals as well as the spectrum entropy of GSR [23] are also used for distress level discrimination.

In addition to the physiological measurements of the drivers, their video-based features are one of the other alternatives for stress, fatigue, alertness, and drowsiness recognition. Video-based features utilized in the literature consist of physical measures of the drivers such as eye movements [23,25–31], head movements [23], and facial expressions [27,32].

Besides the measurements obtained from the driver, mechanical information of vehicle, such as steering-wheel angle, steering wheel motion, speed, deceleration throttle, heading change, throttle, engine performance, and overtaking are also used in some studies [24].

In this paper, a novel feature extraction scheme for drivers' distress level detection is proposed to be implemented in an ITS for increased driving safety. A publicly available dataset of physiological signals collected from automobile drivers by Healey and Picard [15] is obtained from MIT-BIH PhysioNet Multi-parameter Database [33] and used for the verification of the proposed scheme.The proposed feature extraction scheme consists of two phases: firstly, 43-dimensional time-domain statistical feature extraction is performed on the ECG, hand galvanic skin response (hand GSR), foot galvanic skin response (foot GSR), EMG, and RESP signals of each of 10 subjects in the database. Then, in the second phase, dimension reduction of the extracted statistical features is realized by applying Discriminative Common Vector (DCV) decomposition on these features resulting in the proposed subspace feature vector construction. A three-class classification problem is considered for the distress level detection where both the obtained statistical and subspace features are categorized as indicating whether the corresponding driver has low-, moderate-, or high-stress by using Support Vector Machines (SVM) classifier. This paper is concluded with 100 % accuracy by the proposed 2-dimensional feature vector in less time consumption (3421 s) which is extremely important for real-time applications. This outcome shows the superiority of the proposed scheme on the related studies in the literature.

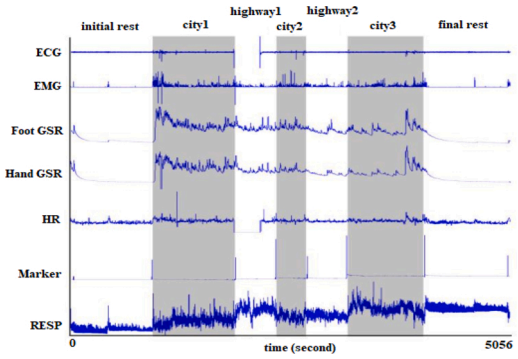

Fig. 2. Measured signals for a sample driver [14].

This paper is organized as follows: the database used and the methods applied in this paper are explained in the following section. The proposed feature extraction scheme is explicitly described in Section 3 wherein the classification procedure and the adopted performance evaluation metrics are also described. The achieved results of the experimental studies and discussions on these results are given in Section 4 while the main conclusions are precisely specified in the last section.

2. Materials & methods

2.1. Database

The ECG, hand GSR, foot GSR, EMG, and RESP signals of automobile drivers collected by Healey and Picard [15] are obtained from MIT-BIH PhysioNet Multi-parameter Database [33] and used in this paper. This dataset includes the ECG, EMG, foot GSR, hand GSR, heart rate (HR), and RESP signals acquired from wearable sensors (Fig. 1) from 17 healthy volunteers while driving from MIT's East Garage to River Street Bridge and back through three cities and two highways. ECG and EMG signals are sampled at 496 and 15.5 Hz, respectively while hand GSR, foot GSR, and RESP signals are sampled at 31 Hz [15].

The driving experiments start with the initial rest and ends by the final rest. The duration of rest states, city drives and highway drives are indicated by a marker in the database. The measurements for driver17 have two parts with durations of 29 and 25 min respectively while the others have durations of 65−93 min. The distress levels of the drivers are determined according to the drive type in the dataset: low stress (during initial and final rest states), moderate stress (during highway drives), and high stress (during city drives). Measured signals for a sample driver are shown in Fig. 2 as an example of the database.

2.2. Discriminative common vectors

Discriminative Common Vectors (DCVs) are introduced by Cevikalp et al. [34] to find a unique DCV for each class in the training data. Given a set of N training data vectors $\vec{x}_i^c$, $i = 1, 2, \cdots, N$ for the c^{th} class of a S -class classification problem, initially, common vector of the c^{th} class is determined by projecting any training data in that class onto the null space of the summation of the individual within-class scatter matrices of all classes, S_w, which is formulized as in Eq. (1), in the DCV algorithm.

$$S_w = \sum_{c=1}^{S} \sum_{i=1}^{N} \left(\vec{X}_i^c - \vec{\mu}^c\right) \cdot \left(\vec{X}_i^c - \vec{\mu}^c\right)^T \quad (1)$$

$\vec{\mu}^c$ in Eq. (1) is the mean of the training data of the c^{th} class and computed as in Eq. (2):

$$\vec{\mu}^c = \frac{1}{N}\cdot\sum_{i=1}^{N}\vec{X}_i^c \tag{2}$$

The difference (Q) and the indifference ($\overline{Q}$) subspaces of S_w are found as the orthonormal eigenvector sets corresponding to the r non-zero and $N-r$ zero eigenvalues of S_w, respectively, where r is the rank of S_w.

$$Q = \left[\vec{e}_1\ \vec{e}_2 \cdots \vec{e}_r\right] \tag{3}$$

$$\overline{Q} = \left[\vec{e}_{r+1}\ \vec{e}_{r+2}\ \cdots\ \vec{e}_N\right] \tag{4}$$

Since the common vector is related to the indifference subspace, common vector of the c^{th} class, $\vec{X}_{com}^c$, can be either obtained by projecting any training data of the c^{th} class onto the indifference subspace of S_w or by subtracting the projection onto the difference subspace of S_w from the data itself, as given in Eq. (5).

$$\vec{X}_{com}^c = \overline{Q}\cdot\overline{Q}^T\cdot\vec{X}_i^c = \vec{X}_i^c - Q\cdot Q^T\cdot\vec{X}_i^c \tag{5}$$

The DCV of any class simply means the projection of its common vector $\vec{X}_{com}^c$ to the difference subspace of the between-class scatter matrix of the common vectors, S_{com}, computed as in Eq. (6) where $\vec{\mu}_{com}$ is the mean of the common vectors and computed as in Eq. (7).

$$S_{com} = \sum_{c=1}^{S}\left(\vec{X}_{com}^c - \vec{\mu}_{com}\right)\cdot\left(\vec{X}_{com}^c - \vec{\mu}_{com}\right)^T \tag{6}$$

$$\vec{\mu}_{com} = \frac{1}{S}\cdot\sum_{c=1}^{S}\vec{X}_{com}^c \tag{7}$$

The difference subspace (W) of the S_{com} is then found as the orthonormal eigenvector set given in Eq. (8) corresponding to the d non-zero eigenvalues of S_{com} where d is the rank of S_{com}.

$$W = \left[\vec{f}_1\ \vec{f}_2\ \cdots\ \vec{f}_d\right] \tag{8}$$

Finally, the DCV of the c^{th} class, $\vec{\Omega}^c$, is obtained by projecting any training data of the c^{th} class onto the difference subspace of S_{com}.

$$\vec{\Omega}^c = W^T\cdot\vec{X}_i^c \tag{9}$$

It should be noted that $\vec{\Omega}^c$ should be unique regardless of which training data in the c^{th} class is projected onto the difference subspace of S_{com}.

2.3. Support vector machines

Given a set of n training data vectors $\vec{x}_i \in \mathbb{R}^m$ and their corresponding labels $L_i \in \{-1, 1\}$, $i = 1, 2, \cdots, n$ for a two-class classification problem, Support Vector Machines (SVM) focus on constructing an optimum class-separating hyperplane

$$\vec{w}^T\cdot\vec{x}_i + b = 0 \tag{10}$$

by maximizing the distance, $\frac{2}{\|\vec{w}\|}$, between the hyperplane and the support vectors, the nearest training vectors from each class to the hyperplane, where $\vec{w}$ is the normal vector of this hyperplane and b is the bias [35]. The training vectors are classified according to the function

$$y = sgn\left(\sum_{i=1,j=1}^{n} L_i\cdot L_j\cdot\alpha_i\cdot\alpha_j\cdot K\left(\vec{x}_i, \vec{x}_j\right) + b\right) \tag{11}$$

in the training stage, and support vectors are the training data vectors $\vec{x}_i$ satisfying the above equation to be zero [36]. In the testing stage, the test vector $\vec{x}_{test}$ is classified according to the function

$$y_{test} = sgn\left(\sum_{i=1}^{n} L_i\cdot\alpha_i\cdot K\left(\vec{x}_i, \vec{x}_{test}\right) + b\right) \tag{12}$$

where the terms y and y_{test} are the class labels determined by the SVM classifier and $K(\vec{x}_i, \vec{x}_j) = \Phi(\vec{x}_i)\cdot\Phi(\vec{x}_j) = <\Phi(\vec{x}_i)\Phi(\vec{x}_j)>$ is the kernel function [36]. By using an appropriate kernel function, the data is transformed into a higher-dimensional space that is resulted in classifying the nonlinear data [37]. For a linear SVM, the kernel function becomes the dot product of the vectors within this function [36].

Table 1
List of bio-signals'-used drivers.

Record Names				
drive5	drive6	drive7	drive8	drive9
drive10	drive11	drive12	drive15	drive16

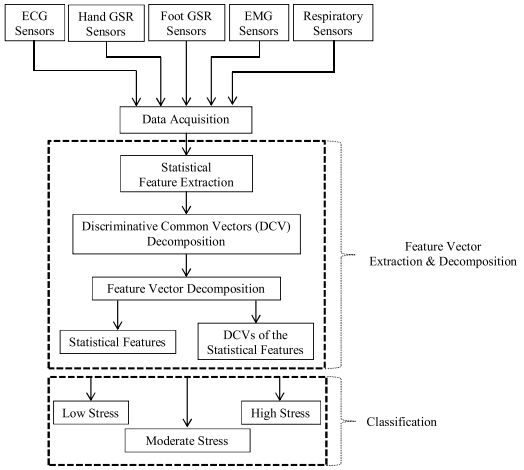

Fig. 3. Block diagram of the proposed study.

3. Experimental study

Some of the drivers have missing signals, and the marker of different driving states is not clear for some of the drivers in the database. Hence, 10 of the 17 drivers' bio-signals are used in this paper. The record names of these 10 drivers are given in Table 1. The initial rest, city drive1, highway drive1, city drive2, highway drive2, city drive3, and final rest durations given by Akbaş [38] are used in this paper.

In this paper, the physiological measurements obtained from ECG, hand GSR, foot GSR, EMG, and RESP sensors are used for distress

Table 2
The mathematical representations of the time-domain statistical features.

Feature	Mathematical Representation
Minimum	$min = minimum\left\{\vec{X}(i)\,\middle|\, i = 1, 2, \cdots N\right\}$
Maximum	$max = maximum\left\{\vec{X}(i)\,\middle|\, i = 1, 2, \cdots N\right\}$
Mean	$\vec{\mu} = \frac{1}{N}\sum_{i=1}^{N}\vec{X}(i)$
Standard Deviation	$\sigma = \sqrt{\frac{1}{N-1}\cdot\sum_{i=1}^{N}\left(\vec{X}(i) - \vec{\mu}\right)^2}$
Median	$med = \vec{X}\left(\frac{N+1}{2}\right)$
Maximum - Minimum	$max - min$
Median - Mean	$\lvert med - \vec{\mu}\rvert$
Skewness	$\frac{1}{\sigma^3}\cdot\sum_{i=1}^{N}\left(\vec{X}(i) - \vec{\mu}\right)^3$
Kurtosis	$\frac{1}{\sigma^4}\cdot\sum_{i=1}^{N}\left(\vec{X}(i) - \mu\right)^4$
Root Mean Square (RMS)	$RMS = \sqrt{mean\left(\vec{X}\cdot\vec{X}^T\right)}$
Root Mean Quad (RMQ)	$RMQ = \sqrt[4]{\left(\vec{X}\cdot\vec{X}^T\right)\cdot\left(\vec{X}\cdot\vec{X}^T\right)^T}$
Zero Crossing Rate (ZCR)	$ZCR = \frac{1}{2N}\cdot\sum_{i=2}^{N}\left(sgn\left(\vec{X}(i)\right) - sgn\left(\vec{X}(i-1)\right)\right)$ $sgn\left(\vec{X}(i)\right) = \begin{cases} 1, \vec{X}(i) \geq 0 \\ -1, \vec{X}(i) < 0 \end{cases}$
Respiration Rate	ZCR of the per minute respiration measurements
Breathing Interval	interval from one respiration (one zero crossing) to another
Breathing Duration (in milliseconds)	$60000\cdot\frac{length(Breathing\ Interval)}{length(1\ minute)}$
Breathing Amplitude	$\lvert Breathing\ Interval\rvert$
Range	$max(Respiration\ Rate) - min(Respiration\ Rate)$

recognition of automobile drivers. The feature extraction stage of this paper consists of two phases. In the first phase, statistical feature extraction of the bio-signals is realized while DCVs of these features are computed in the second phase. Both statistical features and their DCVs (namely, subspace feature vectors) are individually used in the classification stage to determine whether the corresponding driver has low, moderate, or high stress level. The block diagram of the proposed study is given in Fig. 3.

3.1. Feature extraction

Stress measurement through physiological and biological changes includes the measurements of blood pressure, heart beats, reflexes, muscle activity, respiration rate, etc. [9,10]. Hence, feature extraction is realized on ECG, hand and foot GSRs, EMG, and respiratory signals. Since the physiological measurements alter as the stress level alters, statistical feature extraction is executed in order to characterize this alteration in the measurements.

In this stage, the alterations of frequently used time-domain statistical features for Heart Rate (HR), GSR, EMG, and RESP measurements are analyzed, and the most relevant features are determined. The mathematical representations of these most relevant time-domain statistical features, extracted from the N -dimensional per minute signal measurement $\vec{X}$, utilized in this paper are listed in Table 2.

3.2. Feature vector construction

3.2.1. Statistical feature vector construction

The statistical features of all measurements are extracted for each minute, and the resultant feature vector of a driver is constructed as the arithmetic mean of his per minute features.

The statistical HR features, hand GSR, foot GSR, EMG, and RESP features are concatenated to form the definitive 43-dimensional statistical feature vector of each driver given in Table 3. Finally, the feature vector of each driver for each distress level is normalized as given in Eq. (13) to eliminate the domination of high-valued features over other

Table 4
Mathematical representations of the performance evaluation metrics.

Performance Evaluation Metrics	Mathematical Representations
TP: True Positive TN: True Negative FP: False Positive FN: False Negative	
C: Number of classes	N_i: number of data in the i. class
Sensitivity (SNS)	$\%\ SNS = \frac{TP}{TP+FN}\cdot 100$
Specificity (SPC)	$\%\ SPC = \frac{TN}{TN+FP}\cdot 100$
Positive Predictive Value (PPV)	$\%\ PPV = \frac{TP}{TP+FP}\cdot 100$
Negative Predictive Value (NPV)	$\%\ NPV = \frac{TN}{TN+FN}\cdot 100$
False Positive Rate (FPR)	$\%\ FPR = \frac{FP}{FP+TN}\cdot 100$
False Negative rate (FNR)	$\%\ FNR = \frac{FN}{TP+FN}\cdot 100$
False Discovery Rate (FDR)	$\%\ FDR = \frac{FP}{TP+FP}\cdot 100$
False Omission Rate (FOR)	$\%\ FOR = \frac{FN}{TN+FN}\cdot 100$
Accuracy (ACC)	$\%\ ACC = \frac{TP+TN}{TP+TN+FP+FN}\cdot 100$

Table 3
Statistical feature vector construction.

Statistical Feature Vector Construction					
HR Features 6×1	Hand GSR Features 6×1	Foot GSR Features 6×1	EMG Features 9×1	RESP Features 16×1	Statistical Feature Vector 43×1
Maximum Mean Median Standard Deviation Maximum - Minimum Median - Mean	Maximum Mean Median Standard Deviation Maximum - Minimum Median - Mean	Maximum Mean Median Standard Deviation Maximum - Minimum Median - Mean	Maximum Mean Median Standard Deviation Maximum - Minimum Median - Mean Root Mean Square (RMS) Root Mean Quad (RMQ) Zero Crossing Rate (ZCR)	Minimum Respiration Rate Maximum Respiration Rate Average Respiration Rate Standard Deviation of the Respiration Rate Minimum Breathing Duration Maximum Breathing Duration Average Breathing Duration Maximum – Minimum of the Breathing Duration Minimum Breathing Amplitude Maximum Breathing Amplitude Average Breathing Amplitude Maximum – Minimum of the Breathing Amplitude Range Standard Deviation Skewness Kurtosis	$\begin{bmatrix} HR\ Features \\ Hand\ GSR\ Features \\ Foot\ GSR\ Features \\ EMG\ Features \\ RESP\ Features \end{bmatrix}$

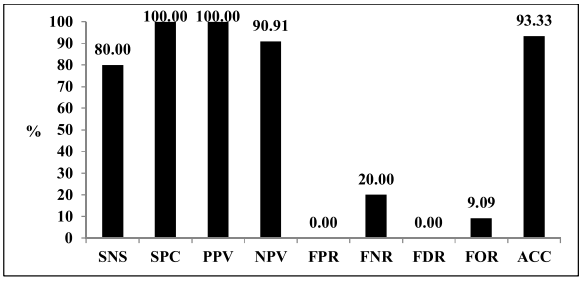

Fig. 4. Average performance evaluation metrics for low stress level obtained using statistical feature vectors.

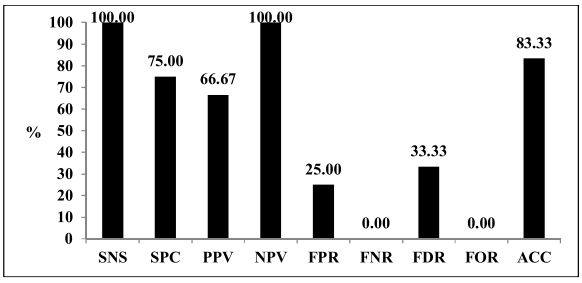

Fig. 5. Average performance evaluation metrics for moderate stress level obtained using statistical feature vectors.

features. The terms $\overrightarrow{\tilde{X}}$, $\overrightarrow{\mu}_{\overrightarrow{X}}$, and $\sigma_{\overrightarrow{X}}$ are the normalized feature vector, the mean, and the standard deviation of the original feature vector $\overrightarrow{X}$, respectively.

$$\overrightarrow{\tilde{X}} = \frac{\overrightarrow{X} - \overrightarrow{\mu}_{\overrightarrow{X}}}{\sigma_{\overrightarrow{X}}} \tag{13}$$

3.2.2. Subspace feature vector construction

DCV of each driver's 43-dimensional statistical feature vector for each distress level is computed, and hence, 2-dimensional subspace feature vectors are obtained.

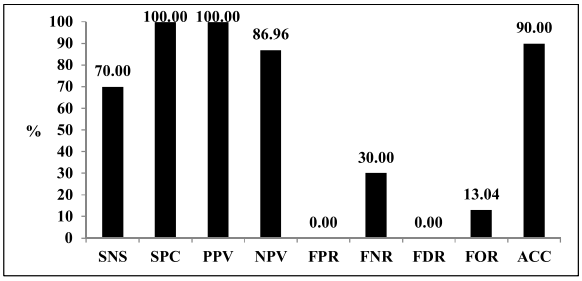

Fig. 6. Average performance evaluation metrics for high stress level obtained using statistical feature vectors.

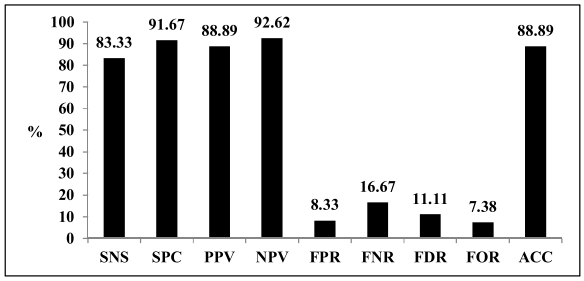

Fig. 7. Overall average performance evaluation metrics using statistical feature vectors.

Table 5
Total confusion matrix obtained in distress recognition using statistical feature vectors.

		Predicted Stress Levels		
		Low	**Moderate**	**High**
Actual Stress Levels	**Low**	8	2	0
	Moderate	0	10	0
	High	0	3	7

3.3. Classification

Stress recognition of automobile drivers is performed using two feature vector construction processes in this paper: statistical and subspace. The linear SVM classifier is used for the categorization of the ten drivers as having low stress, moderate stress, and high stress by using both feature vectors. k -fold cross-validation technique, with $k = 2$, is used for the classification. It means that 5 of 10 drivers (50 %) in each class are used for training while the remaining drivers (50 %) are treated as the test parts in each fold.

3.4. Performance evaluation metrics

The metrics sensitivity (SNS), specificity (SPC), positive predictive value (PPV), negative predictive value (NPV), false positive rate (FPR), false negative rate (FNR), false discovery rate (FDR), false omission rate (FOR), accuracy (ACC) are used for the evaluation of the performance of the proposed system in this study. The mathematical representations of these metrics are given in Table 4. These metrics are computed for each of the two folds, and the averages of the computations are evaluated in

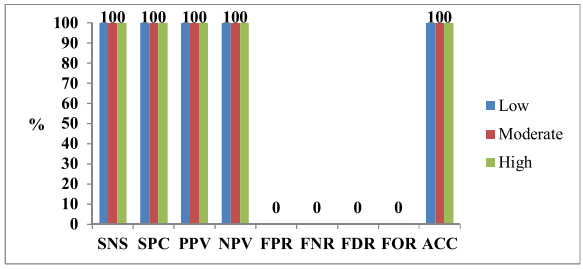

Fig. 8. Average performance evaluation metrics for stress level recognition obtained using subspace feature vectors.

Table 6
Total confusion matrix obtained in distress recognition using subspace feature vectors.

		Predicted Stress Levels		
		Low	Moderate	High
Actual Stress Levels	Low	10	0	0
	Moderate	0	10	0
	High	0	0	10

this paper.

4. Results & discussion

In this paper, distress recognition of automobile drivers is implemented using both statistical and subspace feature vectors. These experiments are performed on a computer with I5−7200U at 2.5 GHz and 8-Gb memory and have been carried out using MATLAB® tool.

Distress recognition is realized by using the statistical feature vectors in the first experiment. Figs. 4–6, show the average performance evaluation metrics for low, moderate, and high stress levels obtained in this experiment, respectively.

The non-100 % SNS, and the 100 % SPC and PPV of low stress level in Fig. 4 indicate the lack of true positives of this class due to the FNs which means that the low stress level is confused to other classes, but none of the other stress levels are classified as low mistakenly.

Analyzing the Fig. 5, it is seen that the moderate stress level is classified by 100 % SNS. The non-100 % PPV and SPC values show the existence of FPs for moderate class indicating that there are drivers suffer from other stress levels but categorized as having moderate stress level.

Like the low stress level, high stress level is confused to other levels, but none of the other distress levels are confused to high stress level as shown in Fig. 6. The overall average performance evaluation metrics obtained by classifying the statistical feature vectors are given in Fig. 7.

The total confusion matrix obtained in distress recognition using statistical feature vectors is given in Table 5. The rows of this matrix indicate the number of drivers in each distress level given based on the ground truth information while the columns show the classified number of drivers in each distress level. Table 5 shows that the mentioned FNs of low and high stress levels belong to the moderate stress levels as well as the FPs of the moderate stress level belongs to the low and high stress levels. This situation explicitly shows that the statistical feature vectors constructed in this paper are directly distinguishable for moderate stress level, and almost distinguishable for the other stress levels. The overall classification sensitivity achieved by using statistical feature vectors is 83.33 % with an accuracy of 88.89 %.

In the second experiment, initially, the same classification process is realized using the 2-dimensional DCVs of the bio-signals. Although the SNS, SPC, PPV, NPV, and ACC metrics are increased to 100 % while FPR, FNR, FDR, and FOR metrics are decreased to 0% in this case, the execution time for feature vector construction using DCV technique is almost 23 times longer than it takes for statistical feature vector construction. Hence, it is proposed to compute the DCVs of the statistical feature vectors and construct subspace feature vectors.

Fig. 8 shows the average performance evaluation metrics for low, moderate, and high stress levels obtained when the subspace feature vectors are tested. This figure shows that the SNS values for both low and high stress levels are increased to 100 % by using the subspace feature vectors. This situation expresses that the novel feature vector, proposed in this paper, eliminates the FNs of the distress levels. Elimination of FNs provides the increment in NPV and ACC to 100 % as well as the decrement in FNR and FOR to 0%. Similarly, it is clearly seen that the SPC of the moderate stress level is also increased to 100 % resulting in removal of FPs by using the proposed feature vector. Hence, the SPC, PPV, and ACC are also increased to 100 % due to 0-FPs while the FPR and FDR are decreased to 0%. These results are confirmed on the total confusion matrix, obtained in distress recognition using subspace feature vectors, given in Table 6.

The execution time comparison for all the realized experiments is given in Table 7. The term ‘DCVs’ in the table indicates the discriminative common vectors obtained directly from the bio-signals while subspace feature vectors are the discriminative common vectors obtained from the statistical feature vectors extracted from the bio-signals.

Analysis of average performance metrics achieved by using statistical feature vectors, DCVs, and subspace feature vectors together with Table 7 explicitly shows that usage of the proposed feature set for distress recognition combines the full accuracy and low execution time advantages of using DCVs and statistical feature vectors, respectively. Thereby, full accuracy is satisfied using the proposed feature vector, like when DCVs are used, with an overall speed-up factor of 9.89 to the DCV usage.

The comparison of the results obtained in this paper with the literature is given in Table 8. The statistical feature vectors, constructed in this study, perform with higher accuracies for most of the three-class stress classification studies [10,13,14,17] in Table 8, but with higher dimension. Hence, superiority of subspace feature vectors show itself with 100 % ACC, SNS, and SPC for three-class stress classification with reduced dimensionality. Similar performance (100 % ACC, SNS, and SPC) is satisfied by using higher-dimensional feature vectors for two-class [14,20] and three-class [39] stress classification studies in Table 8. In the author’s previous work [39], a correlation-based feature selection on a well-known feature set for drivers’ distress recognition is examined. By this feature selection scheme, a 6-dimensional feature vector is constructed for each driver. Then, the classification stage is realized by performing linear SVM, k-Nearest Neighbor (k-NN, $k = 5$), Decision Tree (DT), Random Forest (RF), and Logistic Linear (LLC) classifiers by using 5-fold cross-validation technique. In conclusion, drivers’ distress recognition is succeeded by an ACC, SNS, and SPC of 95.56 %, 93.33 %, and 96.67 %, respectively when linear SVM and LLC

Table 7
The execution time comparison for all the realized experiments.

Total Execution Time (seconds)								
Feature Vector Construction			Classification			Overall		
Statistical Feature Vectors	DCVs	Subspace Feature Vectors	Statistical Feature Vectors	DCVs	Subspace Feature Vectors	Statistical Feature Vectors	DCVs	Subspace Feature Vectors
1.354	31.751	1.381	6030	2.095	2.039	7384	33.846	3.421

Table 8
Comparison of the proposed system with the literature.

Reference	Number of Drivers	Stress Levels	Feature Extraction	Feature Selection/ Reduction	Dimension of the Feature Vector	Classifier	Performance Evaluation
[21]	9	2 stress levels: moderate, high 2 stress levels: low, high	ECG (5-dimensional) Hand GSR (5-dimensional) Foot GSR (5-dimensional) EMG (1-dimensional) RESP (3-dimensional)	Exhaustive Feature Selection	7	Naïve Bayes	ACC: 72.1 % ACC: 87.3 %
[17]	10	3 stress levels: low, moderate, high	ECG (3-dimensional) Hand GSR (6-dimensional) Foot GSR (6-dimensional) EMG (1-dimensional) RESP (6-dimensional)	Principal Component Analysis (PCA)	5	SVM	ACC: 79.13 %
[13]	4	3 stress levels: low, moderate, high	ECG (1-dimensional) Hand GSR (1-dimensional) Foot GSR (1-dimensional) RESP (1-dimensional)	Correlation Analysis	4	Artificial Neural Networks	ACC: 83.44 %
[14]	10	3 stress levels: low, moderate, high 2 stress levels: low, high	ECG (8-dimensional)	–	8 1 8	Naïve Bayes, Logistics, Multi-Layer Perceptron, IBK, J48, Random Forest, Random Tree	ACC: 85.71 % ACC: 85.71 % ACC: 100 %
[10]	10	3 stress levels: low, moderate, high	ECG (3-dimensional) Hand GSR (6-dimensional) Foot GSR (6-dimensional) EMG (1-dimensional) RESP (6-dimensional)	Performance and Cognitive Diversity	11	Combinational Fusion Analysis	ACC: 87.31 %
[16]	10	4 stress levels: low, neutral, high, very high	ECG (2-dimensional) GSR (6-dimensional) EMG (2-dimensional) RESP (2-dimensional) ECG (3-dimensional)	Sequential Forward Floating Selection	7	k-Nearest Neighbor	ACC: 88.6 %
[15]	3	3 stress levels: low, moderate, high	Hand GSR (6-dimensional) Foot GSR (6-dimensional) EMG (1-dimensional) RESP (6-dimensional)	–	22	Fisher Projection and Linear Discriminant Analysis	ACC: 97.4 %
[22]	14	3 stress levels: low, moderate, high	ECG (9-dimensional) Hand GSR (8-dimensional) Foot GSR (8-dimensional) RESP (5-dimensional)	SBL SBL-PCA		SVM	SNS: 99 % SNS: 98 %
[20]	14	2 stress levels: low, high	ECG EMG	–	23	SVM	ACC: 100 % SNS: 100 % SPC: 100 %
[39]	10	3 stress levels: low, moderate, high	ECG (19-dimensional) Hand GSR (20-dimensional) Foot GSR (20-dimensional) EMG (4-dimensional) RESP (23-dimensional)	Correlation Analysis	6	SVM, Logistic Linear Classifier k-Nearest Neighbor, Decision Tree, Random Forest	ACC: 95.56 % FPR: 3.33 % ACC: 100 % FPR: 0%
Proposed system	10	3 stress levels: low, moderate, high	ECG (6-dimensional) Hand GSR (6-dimensional) Foot GSR (6-dimensional) EMG (9-dimensional) RESP (16-dimensional)	DCV	2	SVM	ACC: 100 % SNS: 100 % SPC: 100 %

classifiers are executed. The misclassifications of these classifiers are determined to belong to low and moderate stress levels while the other classifiers (5-NN, DT, and RF) achieved 100 % ACC, SNS, and SPC in the study. It is clearly seen that the misclassifications of low and moderate stress levels detected by linear SVM and LLC classifiers are overcome by using the proposed subspace-based feature vectors. Moreover, computational time for subspace-based feature vector construction of each driver (~0.138 s) is nearly six-thousandth of the one computed in the previous work (~25.305 s) [39].

5. Conclusions

Intelligent Transport Systems (ITS) against traffic violations and accidents in new generation vehicles gain importance day by day. This paper proposes an ITS system for detecting the drivers' distress level using a novel and discriminative two-phase subspace-based feature extraction scheme. The proposed system is verified using the electrocardiogram (ECG), hand galvanic skin response (hand GSR), foot galvanic skin response (foot GSR), electromyogram (EMG), and respiration (RESP) signals in the publicly available MIT-BIH PhysioNet Multiparameter Database. In the first phase of the proposed feature extraction scheme, only time-domain statistical features from the mentioned physiological signals are extracted. Although these time-domain statistical features achieved much more accuracy (88.89 %) in the three-class distress classification problem than almost all of the studies in the literature given in Table 8, it may be a disadvantage for real-time applications to construct a 43-dimensional feature vector and realize the classification. Hence, the subspace analysis of these features is proposed in this paper. By performing Discriminative Common Vector (DCV) decomposition on the initially extracted statistical features, 100 % accuracy of three-level-stress recognition is succeeded by utilizing only 2-dimensional feature vectors. This outcome of the proposed system, full accuracy in three stress level discrimination via a much lower dimensional feature space, shows the superiority of the proposed scheme. Besides, the execution time of the proposed system (feature vector construction followed by classification - ~3.421 s) for 10 drivers is decreased to approximately thirteen-thousandth of execution time of the author's previous study (~254.217 s) [39]. This is a conclusion indicating the convenience of the proposed system to be implemented in a real-time ITS.

Declaration of Competing Interest

The authors declare that they have no known competing financial interests or personal relationships that could have appeared to influence the work reported in this paper.

CRediT authorship contribution statement

Idil Isikli Esener: Conceptualization, Methodology, Software, Validation, Formal analysis, Investigation, Writing - original draft, Writing - review & editing, Visualization.

References

[1] H. Selye, Stress without distress, in: G. Serban (Ed.), Psychopathology of Human Adaptation, Springer, Boston, MA, 1976, pp. 137–146, https://doi.org/10.1007/978-1-4684-2238-2_9. ISBN: 978-1-4684-2238-2.

[2] M.N. Rastgoo, B. Nakisa, A. Rakotonirainy, V. Chandran, D. Tjondronegoro, A critical review of proactive detection of driver stress levels based on multimodal measurements, ACM Comput. Surv. 51 (2018) 1–35, https://doi.org/10.1145/3186585.

[3] L.H. Miller, A.D. Smith, L. Rothstein, The Stress Solution: An Action Plan to Manage the Stress in Your Life, reprint ed., Pocket Books, New York, 1994. ISBN: 978-1501152405.

[4] D.J. Beirness, Do we really drive as we live? The role of personality factors in road crashes, Alcohol Drugs Driving 9 (1993) 129–143.

[5] F. Simon, C. Corbett, Road traffic off ;ending, stress, age, and accident history among male and female drivers, Ergonomics 39 (5) (1996) 757–780.

[6] H. Wiberg, E. Nilsson, P. Lindén, B. Svanberg, L. Poom, Physiological responses related to moderate mental load during car driving in feld conditions, Biol. Psychol. 108 (2015) 115–125, https://doi.org/10.1016/j.biopsycho.2015.03.017.

[7] C. Frasson, P.O. Brosseau, T.H.D. Tran, Virtual environment for monitoring emotional behavior in driving, in: S. Trausan-Matu, K.E. Boyer, M. Crosby, K. Panourgia (Eds.), Intelligent Tutoring Systems, Springer, Cham, 2014, pp. 75–83.

[8] J.G.P. Rodrigues, M. Kaiseler, A. Aguiar, J.P.S. Cunha, J. Barros, A mobile sensing approach to stress detection and memory activation for public bus drivers, IEEE Trans, Intell. Transp. Syst. 16 (2015) 3294–3303, https://doi.org/10.1109/TITS.2015.2445314.

[9] Y. Turunç, Fabrika İşçilerinde Stres Kaynakları Ve Stresle Başa Çıkma Yöntemleri (Unpublished Master's Thesis), Retrieved from, University of Trakya, Institute of Health Sciences, Edirne, Turkey, 2009, http://dspace.trakya.edu.tr/xmlui/handle/1/697.

[10] Y. Deng, Z. Wu, C.H. Chu, Q. Zhang, D.F. Hsu, Sensor feature selection and combination for stress identification using combinatorial fusion, Int. J. Adv. Robot. Syst. 10 (8) (2013), https://doi.org/10.5772/56344.

[11] C.D. Katsis, N. Katertsidis, G. Ganiatsas, D.I. Fotiadis, Toward emotion recognition in car-racing drivers: a biosignal processing approach, IEEE Trans. Syst. Man, Cybern. Part ASystems Humans. 38 (3) (2008) 502–512, https://doi.org/10.1109/TSMCA.2008.918624.

[12] G. Rigas, C.D. Katsis, P. Bougia, D.I. Fotiadis, A reasoning-based framework for car driver's stress prediction, 2008 Mediterr. Conf. Control Autom. - Conf. Proceedings, MED'08 (2008) 627–632, https://doi.org/10.1109/MED.2008.4602162.

[13] M. Singh, A. Bin Queyam, A novel method of stress detection using physiological measurements of automobile drivers, Int. J. Electron. Eng. 5 (2) (2013) 13–20.

[14] N. Keshan, P.V. Parimi, I. Bichindaritz, Machine learning for stress detection from ECG signals in automobile drivers, Proc. - 2015 IEEE Int. Conf. Big Data, IEEE Big Data 2015 (2015) 2661–2669, https://doi.org/10.1109/BigData.2015.7364066.

[15] J.A. Healey, R.W. Picard, Detecting stress during real-world driving tasks using physiological sensors, IEEE Trans, Intell. Transp. Syst. 6 (2) (2005) 156–166, https://doi.org/10.1109/TITS.2005.848368.

[16] J. Healey, R. Picard, SmartCar: Detecting Driver Stress, vol. 4, 2002, pp. 218–221, https://doi.org/10.1109/icpr.2000.902898.

[17] Y. Deng, Z. Wu, C.H. Chu, T. Yang, Evaluating feature selection for stress identification, Proc. 2012 IEEE 13th Int. Conf. Inf. Reuse Integr. IRI 2012 (2012) 584–591, https://doi.org/10.1109/IRI.2012.6303062.

[18] R.R. Singh, S. Conjeti, R. Banerjee, A comparative evaluation of neural network classifiers for stress level analysis of automotive drivers using physiological signals, Biomed. Signal Process. Control 8 (6) (2013) 740–754, https://doi.org/10.1016/j.bspc.2013.06.014.

[19] J.S. Wang, C.W. Lin, Y.T.C. Yang, A k-nearest-neighbor classifier with heart rate variability feature-based transformation algorithm for driving stress recognition, Neurocomputing. 116 (2013) 136–143, https://doi.org/10.1016/j.neucom.2011.10.047.

[20] K. Soman, A. Sathiya, N. Suganthi, Classification of stress of automobile drivers using radial basis function kernel support vector machine, 2014 Int. Conf. Inf. Commun. Embed. Syst. ICICES 2014 (2015) 1–5, https://doi.org/10.1109/ICICES.2014.7034000.

[21] S. Ollander, C. Godin, S. Charbonnier, A. Campagne, Feature and Sensor Selection for Detection of Driver Stress, 2016, pp. 115–122, https://doi.org/10.5220/0005973901150122.

[22] L. Chen, Y. Zhao, P. Ye, J. Zhang, J. Zou, Detecting driving stress in physiological signals based on multimodal feature analysis and kernel classifiers, Expert Syst. Appl. 85 (2017) 279–291, https://doi.org/10.1016/j.eswa.2017.01.040.

[23] G. Rigas, Y. Goletsis, P. Bougia, D.I. Fotiadis, Towards driver's state recognition on real driving conditions, Int. J. Veh. Technol. 2011 (2011) 1–14, https://doi.org/10.1155/2011/617210.

[24] G. Rigas, Y. Goletsis, D. Fotiadis, Real-time driver's stress event detection, IEEE Trans, Intell. Transp. Syst. 13 (1) (2012) 221–234, https://doi.org/10.1109/TITS.2011.2168215.

[25] T. Azim, M.A. Jaffar, A.M. Mirza, Fully automated real time fatigue detection of drivers through Fuzzy Expert Systems, Appl. Soft Comput. 18 (2014) 25–38, https://doi.org/10.1016/j.asoc.2014.01.020.

[26] B. Cyganek, S. Gruszczyński, Hybrid computer vision system for drivers' eye recognition and fatigue monitoring, Neurocomputing 126 (2014) 78–94, https://doi.org/10.1016/j.neucom.2013.01.048.

[27] I. García, S. Bronte, L.M. Bergasa, J. Almazán, J. Yebes, Vision-based drowsiness detector for real driving conditions, Proc. - 2012 IEEE Intelligent Vehicles Symposium (2012) 618–623, https://doi.org/10.1109/IVS.2012.6232222.

[28] D. González-Ortega, F.J. Díaz-Pernas, M. Antón-Rodríguez, M. Martinez-Zarzuela, J.F. Diez-Higuera, Real-time vision-based eye state detection for driver alertness monitoring, Pattern Anal. Appl. 16 (3) (2013) 285–306, https://doi.org/10.1007/s10044-013-0331-0.

[29] J. Jo, S.J. Lee, K.R. Park, I.J. Kim, J. Kim, Detecting driver drowsiness using feature-level fusion and user-specific classification, Expert Syst. Appl. 41 (4) (2014) 1139–1152, https://doi.org/10.1016/j.eswa.2013.07.108.

[30] W. Zhang, B. Cheng, Y. Lin, Driver drowsiness recognition based on computer vision technology, Tsinghua Sci. Technol. 17 (3) (2012) 354–362, https://doi.org/10.1109/TST.2012.6216768.

[31] M. Pedrotti, M.A. Mirzaei, A. Tedesco, J.-R. Chardonnet, F. Mérienne, S. Benedetto, T. Baccino, Automatic stress classifcation with pupil diameter analysis, Int. J. Hum-Comput. Int. 30 (83) (2014) 220–236, https://doi.org/10.1080/10447318.2013.848320.

[32] C.D. Katsis, Y. Goletsis, G. Rigas, D.I. Fotiadis, A wearable system for the aff ;ective monitoring of car racing drivers during simulated conditions, Transport. Res. C-Emer. 19 (3) (2011) 541–551, https://doi.org/10.1016/j.trc.2010.09.004.

[33] A.L. Goldberger, L.A.N. Amaral, L. Glass, J.M. Hausdorff, Ivanov PCh, R.G. Mark, J. E. Mietus, G.B. Moody, C.-K. Peng, H.E. Stanley, PhysioBank, PhysioToolkit, and PhysioNet: components of a new research resource for complex physiologic signals, Circulation 101 (23) (2000) e215–e220 [Circulation Electronic Pages; http://circ.ahajournals.org/cgi/content/full/101/23/e215]; 2000 (June 13).

[34] H. Cevikalp, M. Neamtu, M. Wilkes, A. Barkana, Discriminative common vectors for face recognition, IEEE Trans. Pattern Anal. Mach. Intell. 27 (1) (2005) 4–13, https://doi.org/10.1109/TPAMI.2005.9.

[35] O. Chapelle, P. Haffner, V.N. Vapnik, Support vector machines for histogram-based image classification, IEEE Trans. Neural Netw. 10 (5) (1999) 1055–1064, https://doi.org/10.1109/72.788646.
[36] Y. Ma, W. Chen, X. Ma, J. Xu, X. Huang, R. Maciejewski, Anthony K.H. Tun, EasySVM: a visual analysis approach for open-box support vector machines, Comp. Visual Media 3 (2) (2017) 161–175, https://doi.org/10.1007/s41095-017-0077-5.
[37] K. Özkan, S. Ergin, Ş. Işık, İ. Işıklı, A new classification scheme of plastic wastes based upon recycling labels, Waste Manag. 35 (2015) 29–35, https://doi.org/10.1016/j.wasman.2014.09.030.
[38] A. Akbaş, Evaluation of the physiological data indicating the dynamic stress level of drivers, Sci. Res. Essays 6 (2) (2011) 430–439, https://doi.org/10.5897/SRE10.943.
[39] İ. Işıklı Esener, A novel stress-level-specific feature ensemble for drivers' stress level recognition, BSEU J. Sci. 6 (1) (2019) 12–23, https://doi.org/10.35193/bseufbd.554791.